Results in Engineering 29 (2026) 109404

Contents lists available at ScienceDirect

Results in Engineering

journal homepage: www.sciencedirect.com/journal/results-in-engineering

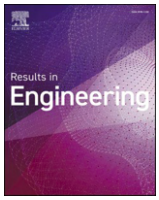

Research paper

Uplift resistance of winged composite piles with surplus soil backfill: Model experiments and numerical validation

Shinya Inazumi [a,*], Yusuke Watanabe [b], Yosuke Mizutani [c], Yoshihiro Matsuo [d], Ken-ichi Shishido [e]

[a] College of Engineering, Shibaura Institute of Technology, Tokyo 135-8548, Japan
[b] Nissin Co. Ltd., Tokyo 166-0002, Japan
[c] Kanematsu Sustech Corporation, Tokyo 103-0007, Japan
[d] Saitama Yae Industries Co. Ltd., Saitama 367-0206, Japan
[e] Tomec Corporation, Ibaraki 306-0314, Japan

ARTICLE INFO

Keywords:
Winged composite pile foundation
Model experiment
Uplift resistance
Construction surplus soil
Expanded base wing
Numerical validation
Sustainable construction

ABSTRACT

This study presents a comprehensive experimental and numerical investigation of uplift resistance characteristics in winged composite pile foundations designed to utilize construction surplus soil, addressing Japan's critical construction waste management challenges where on-site utilization remains at only 54.3%. The novel composite system integrates steel structural members (liner plates) surrounding steel pipe piles with expanded base wings, with the annular space filled with construction surplus soil. Through 35 model-scale uplift tests examining seven distinct configurations, the study systematically evaluated effects of steel structural member presence, soil density variations (12 and 15 kN/m^3), and surface irregularities across five expanded base wing diameters (32–64 mm). Results demonstrate that uplift resistance increases proportionally with expanded base wing diameter across all configurations, with the composite system achieving performance comparable to or exceeding conventional steel pipe piles under optimal conditions. Soil density emerged as a critical parameter, with 20% density reduction causing approximately 50% decrease in uplift resistance, emphasizing the importance of compaction quality control. Corrugated steel structural members enhanced resistance by 12–13% through improved frictional engagement. Finite element method analyses of three selected cases validated experimental trends, confirming qualitative agreement despite quantitative differences attributable to simplified material parameters. The study provides integrated design guidelines combining experimental and numerical findings, contributing to practical implementation of winged composite pile foundations for wind-load-resistant structures while achieving substantial utilization of construction surplus soil, thereby addressing both structural and environmental imperatives in geotechnical engineering.

1. Introduction

1.1. Study background and motivation

Structures such as transmission towers and radio towers experience significant wind loads, requiring pile foundations with substantial uplift resistance to withstand uplift forces generated by lateral loading. Recent climate change has intensified these requirements, with increased typhoon severity and tornado frequency elevating wind loads on such structures [1–5]. This trend necessitates development of pile foundations with enhanced uplift resistance capacity.

In response to increasing environmental loads, a wide range of experimental and numerical studies have examined the uplift and pullout behavior of foundations for towers, monopoles, and solar array structures in granular and composite soils [1–5]. These studies have clarified key mechanisms, such as the development of conical failure surfaces and the influence of group interaction effects and soil reinforcement or anchorage geometry on ultimate pullout resistance. However, most of this research has concentrated on conventional pile or anchor geometries in natural or cement-improved soils. There has been limited consideration of foundation systems designed to handle large amounts of excess construction soil while increasing uplift capacity.

* Corresponding author.
E-mail address: inazumi@shibaura-it.ac.jp (S. Inazumi).

https://doi.org/10.1016/j.rineng.2026.109404
Received 16 November 2025; Received in revised form 8 January 2026; Accepted 1 February 2026
Available online 1 February 2026

Simultaneously, Japan faces critical challenges in construction surplus soil management. According to the Ministry of Land, Infrastructure, Transport and Tourism's Construction By-products Survey (January 2020), while construction waste achieves 97.2% recycling and reduction rate, construction surplus soil demonstrates only 79.8% effective utilization, with on-site utilization at merely 54.3% [6,7]. With annual generation of approximately 290 million m^3 and off-site disposal of 130 million m^3, inadequate management practices have led to environmental pollution and landslide risks, creating significant societal concerns [8,9]. Enhancing on-site utilization rates, particularly through technologies capable of utilizing large volumes of lower-quality surplus soil, represents an urgent priority for the construction industry [10,11].

1.2. Review of existing technologies and study gap

Traditional pile foundation systems have evolved to resist uplift through several approaches, including belled or enlarged base piles, grouted or planted piles, anchor piles, and composite foundations [12–15]. Enlarged base or belled piles increase bearing resistance by enlarging the base area and have been widely studied under compressive and tensile loading conditions. Grouted or planted piles and anchor piles further enhance uplift resistance by improving the pile-soil interface and enlarging the effective failure surface through base grouting or mechanical anchorage. Soil-cement column systems and cement-improved ground around piles can increase lateral and pullout resistance; however, they generally require substantial cement consumption and high-quality backfill materials.

Concurrently, numerous recent studies have investigated various composite or hybrid pile systems, including pile-net composite foundations, soil-filling piles with spiral or fin-type attachments, and hybrid steel-concrete or GFRP pile foundations, to enhance axial and lateral performance. These contributions demonstrate that a rational combination of steel members, concrete, grout, and surrounding ground can significantly improve foundation performance under complex loading conditions. However, most of these composite systems are not designed to utilize large quantities of construction surplus soil, and their design frameworks rarely incorporate environmental or waste management objectives [6–11].

The critical study gap emerges at the intersection of structural performance requirements and sustainable construction practices [16–20]. Existing technologies lack systematic integration of structural performance enhancement with large-volume construction surplus soil utilization. Previous study has examined individual aspects of pile behavior under uplift loading or soil improvement techniques separately, but no comprehensive experimental study has examined how steel structural member configurations, soil density variations, and surface characteristics collectively influence uplift resistance in composite systems designed specifically for surplus soil application. This gap is particularly significant considering the growing regulatory pressure to reduce construction waste disposal and the policy targets aimed at improving the on-site utilization of excavated soils. Additionally, the structural demands imposed by climate change-intensified wind loads must be considered [1–11,16–20].

1.3. Novelty and originality of this study

This study presents three fundamental innovations that address the identified study gap. First, the novel winged composite pile foundation system introduces a unique structural configuration integrating steel structural members such as liner plates with expanded-base steel pipe piles, creating an annular space specifically engineered for construction surplus soil placement. This configuration fundamentally differs from existing technology by accommodating lower-quality surplus soil while maintaining structural performance through the synergistic interaction between the steel elements and contained soil mass. The system achieves dual functionality by simultaneously enhancing structural resistance and advancing environmental sustainability through massive surplus soil utilization [21–23].

Second, the study employs a comprehensive parametric experimental investigation examining seven distinct test configurations that systematically vary steel member presence, soil density differences both internal and external to structural members, and surface irregularities. The statistical rigor of conducting 35 model-scale tests with five expanded base wing diameters per configuration establishes robust performance relationships across the full parameter space. This unprecedented scope represents the first systematic evaluation of winged composite pile foundation uplift resistance characteristics considering multiple interacting parameters simultaneously [16].

Third, the integrated experimental-numerical validation framework provides bidirectional confirmation of observed phenomena through finite element method analyses of three selected cases. This integration of experimental findings and numerical predictions into practical design guidelines enables direct translation of study findings to field implementation protocols, bridging the gap between laboratory investigation and engineering practice [24–26].

1.4. Study objectives

This study aims to experimentally investigate uplift resistance characteristics of winged composite pile foundations utilizing construction surplus soil through model-scale testing and numerical validation. The study seeks to quantify the effects of key design parameters including steel structural member presence or absence, soil density variations comparing 15 kN/m^3 versus 12 kN/m^3 conditions, steel member surface characteristics distinguishing smooth from corrugated configurations, and expanded base wing diameter ranging from 32 to 64 mm. Beyond parameter quantification, the study establishes performance relationships between expanded base wing diameter and uplift resistance under various configurations, validates experimental findings through finite element method numerical reproduction analyses, develops practical design guidelines integrating experimental and numerical insights for field implementation, and demonstrates the feasibility of utilizing construction surplus soil in structural foundations while maintaining adequate uplift resistance for wind-loaded structures [16,27,13].

2. Winged composite pile foundation system

2.1. Structural configuration

Fig. 1 illustrates the plan view and cross-section of the developed winged composite pile foundation system. This innovative structural form differs fundamentally from conventional pile foundations through its capacity for large-volume construction surplus soil utilization [28,29]. The system comprises four primary components working synergistically to resist uplift forces while incorporating site-generated surplus soil.

Steel structural members, implemented using cylindrical elements such as liner plates [30], create subsurface voids within the ground mass. These members serve dual functions by retaining construction surplus soil against lateral earth pressures while simultaneously developing frictional resistance with surrounding ground during uplift loading. The selection of liner plates or similar corrugated members enhances this frictional interaction through increased surface area and mechanical interlocking with contained soil.

An expanded-base steel pipe pile with a disk-shaped wing at the pile tip is positioned centrally within the steel structural member. The expanded base provides the primary bearing resistance mechanism against uplift forces, mobilizing the strength of both the natural ground below and the contained surplus soil above through bearing pressure distribution. The sizing of this expanded base wing relative to the steel structural member diameter emerges as a critical design parameter

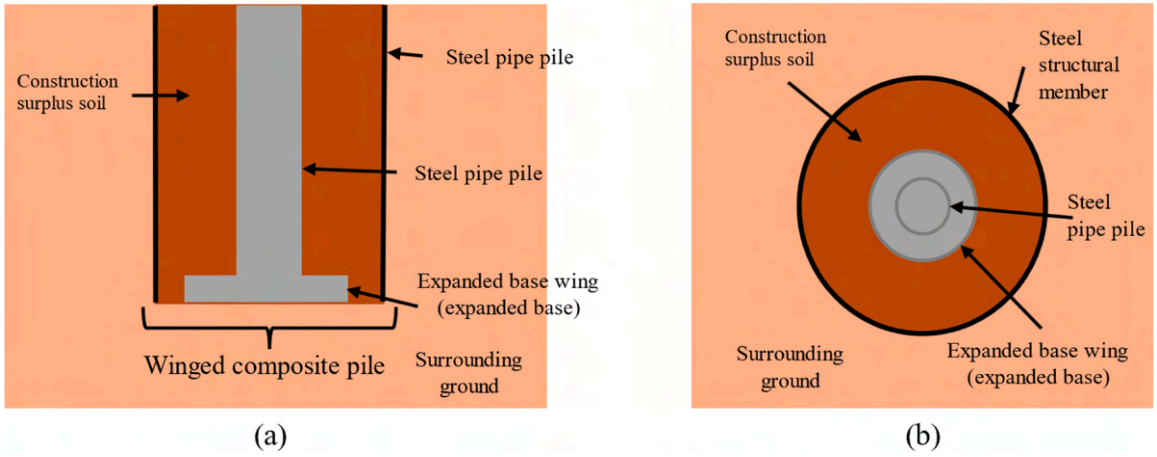

Fig. 1. (a) Cross-sectional and (b) plan views of winged composite pile foundation.

governing overall system performance.

Construction surplus soil excavated during site preparation fills the annular space between the steel pipe pile and structural member. This soil, rather than representing waste requiring disposal, becomes an integral structural component working in conjunction with the expanded base wing to resist uplift forces. The transformation of surplus soil from

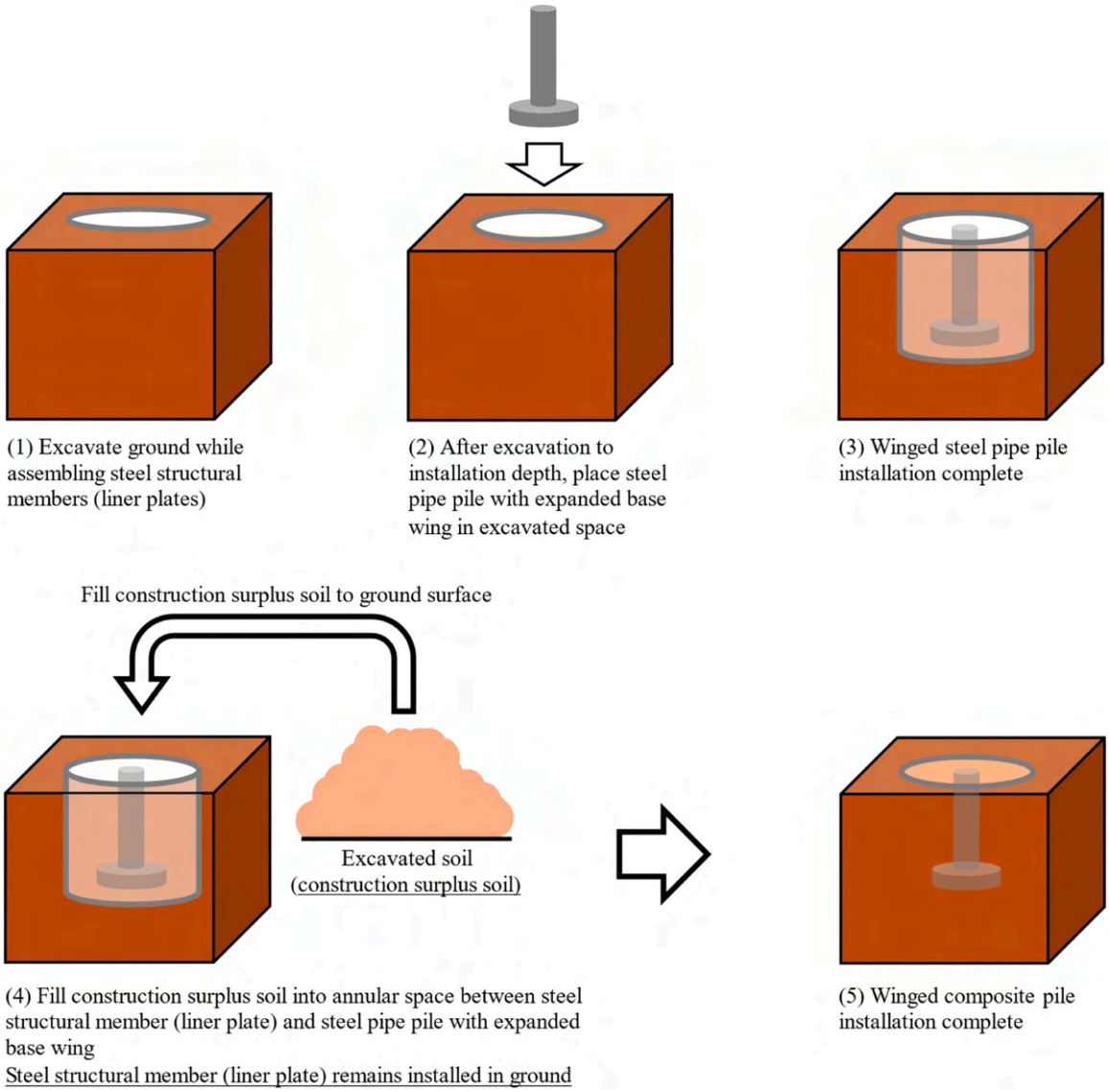

. 2. Construction sequence for winged composite pile foundation.

waste material to structural element represents the key innovation enabling both structural performance and environmental sustainability.

When site conditions or performance requirements dictate, cement-based solidification agents can be mixed with construction surplus soil near the expanded base wing to enhance local strength. This optional treatment provides design flexibility for accommodating particularly poor quality surplus soils or demanding loading conditions while still maintaining the fundamental concept of surplus soil utilization [31–33].

This configuration enables construction surplus soil to form an integrated mass with the pile's expanded base wing, creating a unified resistance mechanism against uplift forces. The steel structural member not only retains soil but also contributes to uplift resistance through friction with surrounding ground, distinguishing this system from conventional approaches that rely solely on pile-ground interaction.

2.2. Construction methodology

Fig. 2 illustrates the construction sequence for winged composite pile foundations, which has been developed to facilitate efficient on-site implementation while maximizing surplus soil utilization. The construction procedure comprises the following sequential steps:

- Step 1 (Ground Excavation): Excavation proceeds to the specified depth with diameter slightly larger than the steel structural member outer diameter to facilitate member installation while minimizing soil disturbance in surrounding ground.
- Step 2 (Steel Structural Member Installation): Steel structural members are installed within the excavated hole using procedures adapted to the specific member type. When employing liner plates, the members can be assembled and installed progressively during excavation, enabling efficient construction in variable ground conditions.
- Step 3 (Steel Pipe Pile Placement): The expanded-base steel pipe pile is positioned centrally within the steel structural member using alignment fixtures at the pile head to ensure verticality throughout the soil placement process. Maintaining accurate pile alignment proves critical for achieving design performance.
- Step 4 (Construction Surplus Soil Placement): Construction surplus soil is placed in layers between the steel pipe pile and structural member, with each layer approximately 30 cm thick after compaction. Each layer receives systematic compaction using metal tampers or mechanical compactors, with compaction effort controlled to achieve target soil density.
- Step 5: (Strength Enhancement (Optional)): When design requirements specify strength enhancement, cement-based solidification agents are mixed with construction surplus soil near the expanded base wing during placement of those layers. The extent of soil treatment follows design specifications based on required uplift capacity and surplus soil quality.
- Step 6 (Pile Head Connection): The construction sequence concludes with connection of the steel pipe pile head to the structure foundation, completing load transfer from the superstructure through the pile system to the supporting ground.

This construction methodology enables direct utilization of site-generated construction surplus soil in winged composite pile foundations, substantially reducing off-site disposal volumes while creating a structurally effective foundation system. The practical feasibility of this approach in field conditions represents a key consideration validated through the experimental program described in subsequent sections.

3. Experimental program

3.1. Experimental objectives and overview

The experimental program was designed to achieve two primary objectives: first, to evaluate winged composite pile foundation uplift resistance characteristics experimentally across a comprehensive parameter space, and second, to generate high-quality data enabling validation of numerical analysis results. Tests employed scaled models at 1/50 scale, representing full-scale 15 m pile length as 300 mm models while maintaining geometric similarity for key features including pile diameter, expanded base wing proportions, and steel structural member dimensions.

Seven test configurations were examined, systematically varying steel structural member presence, soil density differences between internal and external regions, and steel member surface irregularities. Each configuration was tested with five different expanded base wing diameters spanning 32, 40, 48, 56, and 64 mm, totaling 35 individual uplift tests. This parametric approach enables isolation of individual parameter effects while establishing their interactions across the performance space relevant to practical design applications.

3.2. Testing apparatus

The testing apparatus comprises three integrated systems: soil container, loading mechanism, and measurement instrumentation. The soil container utilizes acrylic construction with internal dimensions of 400 mm length, 400 mm width, and 600 mm height. Acrylic material selection enables visual observation of ground and pile behavior through container sidewalls during testing, providing qualitative insights into failure mechanisms that complement quantitative load-displacement measurements. Drainage holes incorporated in the container base facilitate soil removal after testing while preventing pore pressure buildup during loading if soil saturation occurs inadvertently.

The loading apparatus, shown in Fig. 3, applies controlled vertical uplift displacement to the pile head through an electric jack system. This displacement-controlled loading approach, as opposed to load-controlled methods, ensures stable post-peak behavior observation and complete load-displacement relationship characterization [34]. The load cell, with 100 N maximum capacity and 0.01 N measurement precision, provides accurate quantification of uplift forces throughout the loading history. The capacity selection reflects the scale model forces expected from preliminary analyses while ensuring adequate resolution for detecting subtle performance differences between configurations.

Measurement instrumentation comprises a laser displacement sensor monitoring pile head displacement with 0.01 mm precision and the load cell measuring uplift force continuously throughout each test. A data logger captures synchronized load-displacement measurements at 1-s intervals, providing temporal resolution adequate for the 0.5 mm/min loading rate employed. This measurement configuration enables precise characterization of both peak resistance and post-peak behavior, with the latter proving particularly important for understanding failure mechanisms and assessing ductility characteristics relevant to structural design.

3.3. Testing procedures

Fig. 4 illustrates the systematic testing procedure developed to ensure reproducibility across the 35-test experimental program. The procedure comprises the following sequential operations:

- Step 1 (Soil Container Preparation): The soil container is positioned horizontally with non-woven geotextile fabric placed on the base to prevent soil loss through drainage holes while permitting pore water drainage.
- Step 2(Steel Structural Member Installation (for winged composite pile cases)): Steel structural members fabricated from PVC pipe or corrugated sheet material (Fig. 5) are installed at the container center before soil placement, using alignment jigs to maintain verticality and concentric positioning.

(a) Overall View (b) Focus on the Loading Section

Fig. 3. Temperature-controlled tensile testing apparatus (Instron tensile compression testing machine (AG-50kNX)).

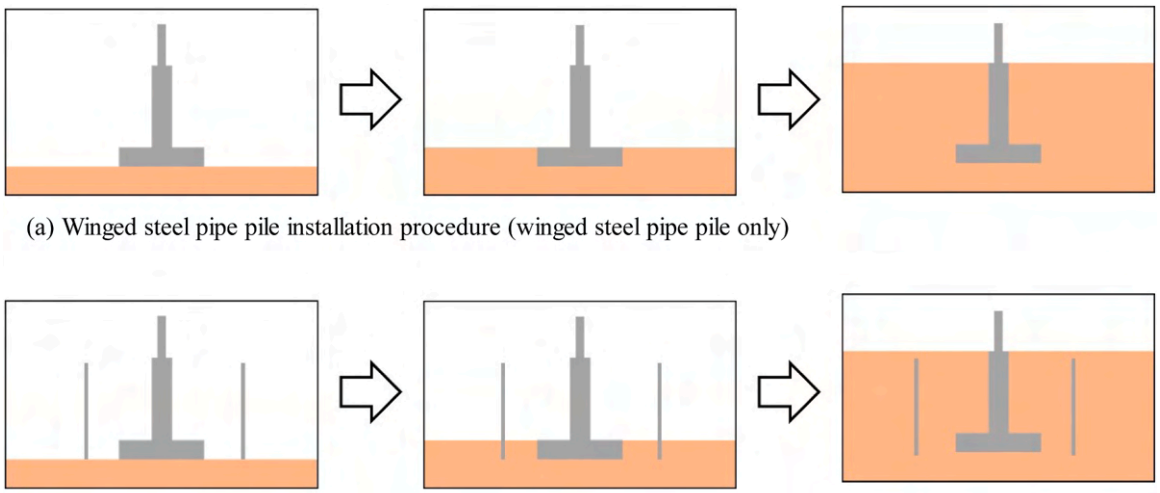

(a) Winged steel pipe pile installation procedure (winged steel pipe pile only)

(b) Winged composite pile installation procedure (winged composite pile configuration)

Fig. 4. Installation procedures for model tests.

(a) Top view of a steel structural member (b) Lateral view of a steel structural member with surface irregularities (c) Oblique view of a steel structural member with surface irregularities

. 5. Steel structural members with surface irregularities.

- Step 3 (Pile Installation): Model steel pipe piles with various expanded base wing diameters (Fig. 6) are placed at the container center, or at the steel member center when such members are present. Fig. 7 shows the 64 mm diameter expanded base wing pile. Fixtures attached to pile heads maintain verticality throughout soil placement.
- Step 4 (Test Soil Placement): Test soil is placed in approximately 50 mm thick layers both outside and inside steel structural members when present. Commercial silica sand No 5 (grain size 0.25–0.5 mm) serves as the test soil. Each layer receives compaction using a metal tamper: 25 blows per layer for 15 kN/m^3 density; 10 blows per layer for 12 kN/m^3 density.
- Step 5 (Instrumentation Installation): Following soil placement completion, the loading apparatus and displacement sensor are installed at the pile head.
- Step 6 (Uplift Loading): Displacement-controlled uplift loading commences at 0.5 mm/min rate continuing to 20 mm maximum displacement. Pile head displacement and load are measured continuously throughout loading.

This systematic approach to experimental execution ensures

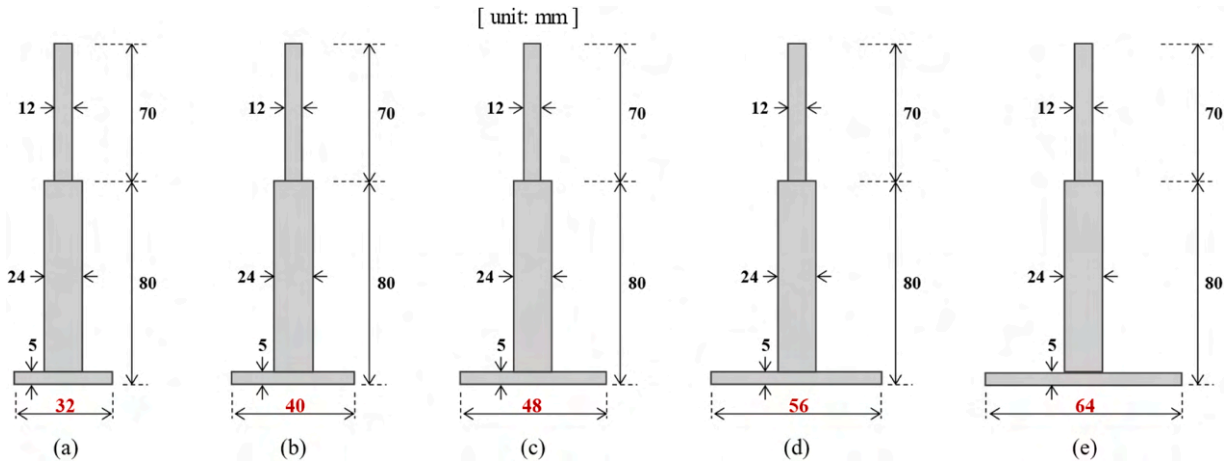

. 6. Dimensions of model steel pipe piles.

. 7. Steel pipe pile with 64 mm expanded base wing.

reproducibility while enabling careful control of key parameters governing uplift resistance behavior.

The internal dimensions of the soil container are 400 mm × 400 mm × 600 mm, corresponding to widths approximately 6.3–12.5 times the 32–64 mm expanded base wing diameter and a depth about 9.4 times the 300 mm model pile length. The uplift mechanism of the winged composite pile is primarily confined to the soil mass inside the steel structural member and the soil immediately surrounding the expanded base wing, as evidenced by post-test observations in Figs. 10 and 11. Consequently, the influence of the container walls on uplift resistance is limited, though some confinement effect is present and consistently included in all test cases.

3.4. Test case matrix

Table 1 summarizes the seven test configurations implemented in this experimental program, with five expanded base wing diameters tested for each case generating the 35-test matrix. Case 1 and Case 2 examine steel pipe pile behavior without steel structural members, representing baseline performance for subsequent comparison with winged composite pile configurations. Case 1 employs 15 kN/m^3 soil density throughout the container while Case 2 reduces density to 12 kN/m^3, enabling isolation of density effects independent of steel member presence.

Table 1
Test case matrix showing configurations.

	Steel Structural Member Presence (Pile Configuration)	Soil Density Inside Steel Member (kN/m^3)	Soil Density Outside Steel Member (kN/m^3)	Steel Member Surface Irregularities
Case 1	Absent (Steel pipe pile only)	15	15	Absent
Case 2	Absent (Steel pipe pile only)	12	12	Absent
Case 3	Present (Winged composite pile)	15	15	Absent
Case 4	Present (Winged composite pile)	12	12	Absent
Case 5	Present (Winged composite pile)	15	15	Present
Case 6	Present (Winged composite pile)	15	12	Absent
Case 7	Present (Winged composite pile)	15	12	Present

Case 3 and Case 4 introduce steel structural members while maintaining uniform soil density both internal and external to these members. Case 3 employs 15 kN/m^3 throughout while Case 4 utilizes 12 kN/m^3 universally. Comparison of these cases with their respective baseline configurations (Cases 1 and 2) quantifies the effects of steel structural member installation on uplift resistance enhancement, addressing a fundamental question regarding winged composite pile performance.

Case 5 maintains identical conditions to Case 3 but substitutes corrugated steel structural members for the smooth members used in Case 3. Direct comparison between these cases isolates the effect of surface irregularities on frictional resistance, addressing practical design questions regarding optimal steel member selection for field applications.

Case 6 and Case 7 introduce density differentials between internal and external regions, with 15 kN/m^3 internally and 12 kN/m^3 externally. This configuration simulates realistic field conditions where construction surplus soil placed within steel structural members may receive different compaction effort or possess different characteristics than surrounding site soils. Case 7 extends Case 6 by employing corrugated rather than smooth steel members, enabling assessment of whether surface irregularity benefits persist under density differential conditions.

Soil volume for each case was meticulously recorded separately for internal and external regions, with mass measurements performed layer-by-layer during placement. This careful mass and volume tracking

ensures experimental soil density reproducibility and enables correlation of measured performance with actual as-built density conditions rather than target values alone.

4. Experimental results and discussion

4.1. Overview of results

Figs. 8 and 9 present comprehensive experimental results across all test configurations. Fig. 8 displays pile head displacement versus uplift force relationships for all seven cases, with each case shown at two displacement scales to capture both initial response characteristics and extended post-peak behavior. Fig. 9 summarizes uplift force versus expanded base wing diameter relationships, consolidating maximum resistance values for direct comparison across cases. Figs. 10 and 11 provide photographic documentation of post-test conditions for Case 3, illustrating physical mechanisms underlying the measured load-displacement responses.

4.2. Baseline performance: Cases 1 and 2

Case 1, representing steel pipe piles in 15 kN/m^3 density soil without steel structural members, establishes baseline performance against which winged composite pile enhancements are evaluated. As shown in Fig. 8(a) and (b), uplift force increases systematically with expanded base wing diameter, progressing from 35.64 N at 32 mm diameter through intermediate values of 47.20 N, 50.20 N, and 53.88 N at 40 mm, 48 mm, and 56 mm respectively, reaching maximum resistance of 58.98 N at 64 mm diameter. The load-displacement relationships show an almost linear initial response up to a displacement of about 1–2 mm. This is followed by a nonlinear region where the uplift resistance quickly approaches its peak and then slowly decreases. This reflects the progressive mobilization and softening of the soil resistance around the expanding deformation zone above the base wing. Following peak load attainment, responses show slight load reduction stabilizing to relatively constant residual resistance, indicating that post-peak behavior remains controlled rather than catastrophic.

Case 2 mirrors Case 1 configuration but reduces soil density to 12 kN/m^3 throughout the container. Fig. 8(c) and (d) reveal similar displacement-response characteristics but substantially reduced uplift forces: 17.75 N, 18.12 N, 19.42 N, 21.26 N, and maximum 28.74 N for the respective expanded base wing diameters. Direct comparison between Cases 1 and 2 quantifies the dramatic influence of soil density on uplift resistance. The 20% density reduction from 15 to 12 kN/m^3 produces approximately 50% reduction in uplift force across all expanded base wing diameters. This substantial sensitivity reflects the combined effects of reduced bearing resistance around expanded base wings and decreased shaft friction along pile surfaces, both of which depend fundamentally on soil density through its influence on stress-dependent strength parameters. These baseline results establish that compaction quality control during construction surplus soil placement will prove critical for achieving design performance in field applications.

4.3. Winged composite pile with uniform density: Cases 3 and 4

Case 3 introduces steel structural members while maintaining 15 kN/m^3 uniform density both internal and external to these members, enabling direct assessment of steel member effects by comparison with Case 1 baseline. Fig. 8(e) and (f) show uplift forces of 36.61 N, 36.04 N, 32.29 N, 41.38 N, and maximum 53.92 N for expanded base wing diameters progressing from 32 to 64 mm. Comparison with Case 1 reveals nuanced behavior: at smaller diameters, Case 3 performs comparably, but at larger diameters, particularly 56 mm and 64 mm, Case 3 exhibits slightly reduced resistance relative to Case 1. This reduction likely results from frictional resistance developing between the soil mass moving upward with the expanded base wing and the steel structural member inner wall, effectively creating additional resistance that must be overcome during uplift. This observation suggests that steel structural member benefits emerge through mechanisms other than simple resistance addition, requiring careful consideration in design.

Case 4 parallels Case 3 configuration but employs 12 kN/m^3 uniform density, enabling evaluation of whether steel structural member effects depend on soil density. Uplift forces of 13.99 N, 17.58 N, 16.63 N, 17.45 N, and maximum 19.32 N demonstrate that winged composite pile behavior persists at reduced density. Comparison with Case 2 baseline reveals interesting trends: Case 4 shows lower resistance at 32 mm diameter but higher resistance at larger diameters. This crossover behavior suggests that steel structural member benefits become more pronounced as expanded base wing diameter increases, possibly because larger diameters create wider zones of soil disturbance that interact more effectively with steel member confinement effects. The consistent increase of uplift resistance with expanded base wing diameter across both Cases 3 and 4 confirms that fundamental design relationships established for conventional piles remain applicable to winged composite pile systems.

4.4. Surface irregularity effects: Case 5

Case 5 maintains identical conditions to Case 3 while substituting corrugated steel structural members for smooth members, isolating surface irregularity effects through direct comparison. Fig. 8(i) and (j) present uplift forces of 37.79 N, 30.40 N, 38.74 N, 41.37 N, and maximum 60.92 N across the diameter range. The maximum value of 60.92 N at 64 mm diameter substantially exceeds the corresponding Case 3 value of 53.92 N, representing approximately 13% enhancement attributable solely to corrugated surface geometry. This performance improvement derives from two complementary mechanisms: increased contact area between construction surplus soil and steel structural member surface, and mechanical interlocking effects wherein irregularities create local bearing resistance against soil movement. The magnitude of enhancement, while modest in percentage terms, translates to significant capacity increases in full-scale applications, potentially enabling reduced pile dimensions or enhanced safety margins for equivalent loading conditions.

The practical implications prove particularly significant for field implementation. Liner plates, commonly employed in temporary excavation support, possess inherent corrugations serving as structural stiffeners. The experimental results demonstrate that these existing corrugations provide substantial secondary benefits for uplift resistance when liner plates serve as permanent steel structural members in winged composite pile foundations. This dual functionality, structural stiffness and enhanced soil interaction, adds no incremental material cost while improving performance, making corrugated members economically attractive for winged composite pile applications.

4.5. Density differential effects: Cases 6 and 7

Case 6 introduces density differential with 15 kN/m^3 internally and 12 kN/m^3 externally, simulating realistic field conditions where construction surplus soil placement and compaction within confined spaces may differ from surrounding site work. Fig. 8(k) and (l) show uplift forces of 19.88 N, 19.62 N, 21.17 N, 22.22 N, and maximum 27.85 N. These values fall between the uniform high-density Case 3 results and uniform low-density Case 4 results, confirming that external soil density influences overall system behavior despite the expanded base wing residing primarily within the internal soil mass. This finding indicates that uplift resistance mechanisms extend

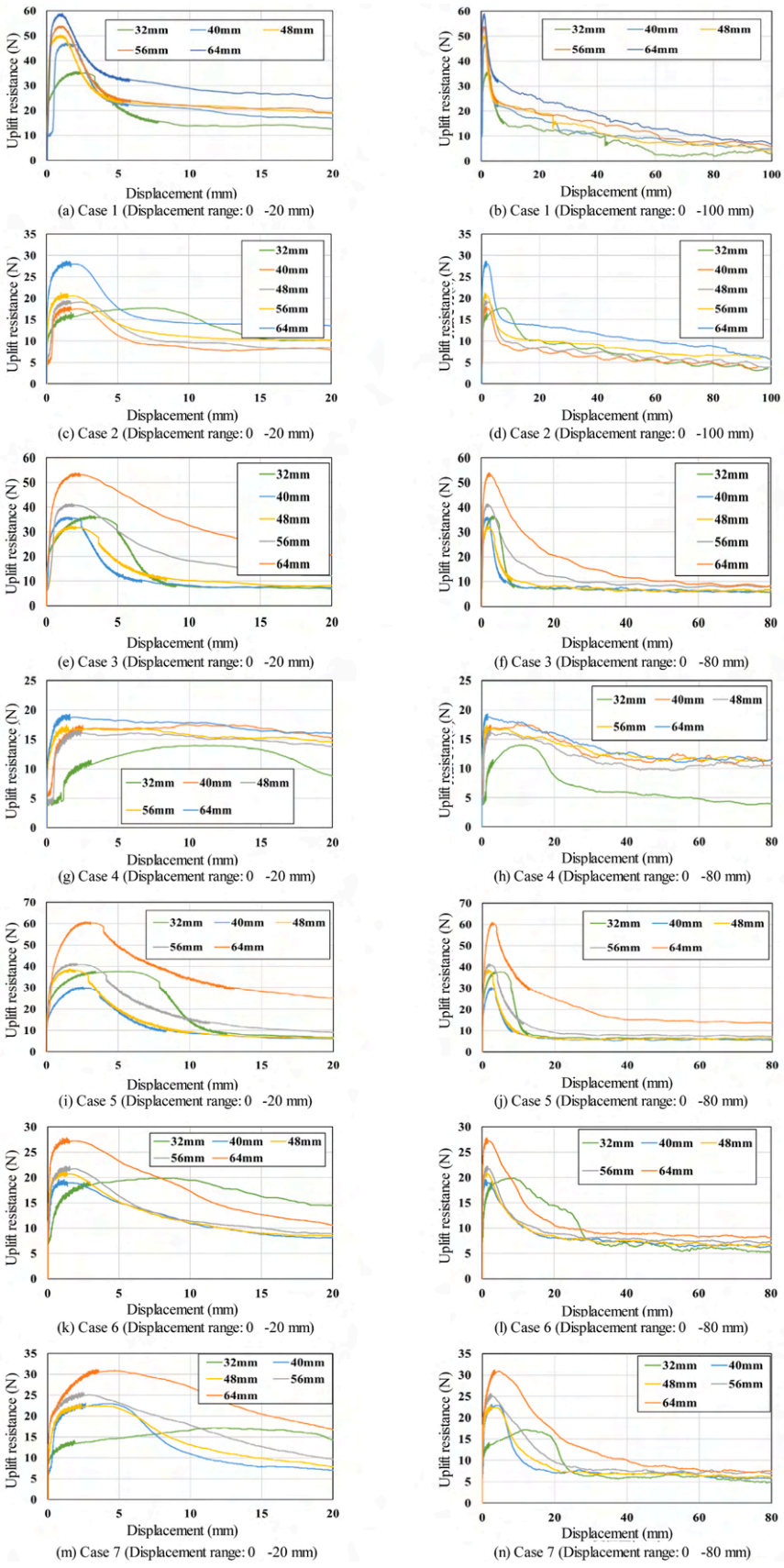

Fig. 8. Load-displacement relationships for all test cases (a-n).

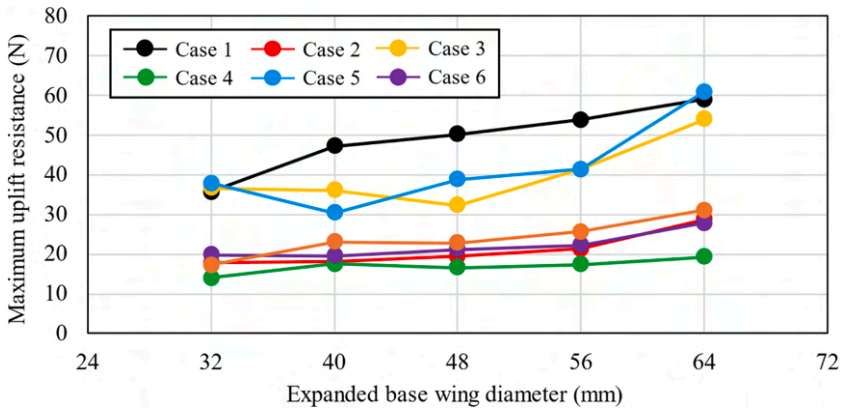

Fig. 9. Maximum uplift resistance versus expanded base wing diameter for all cases.

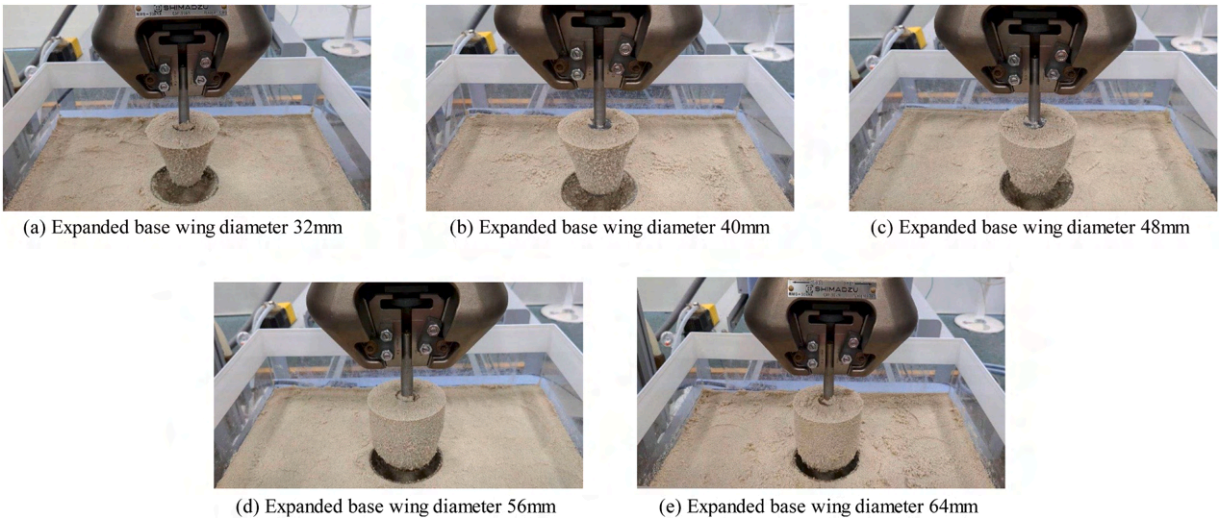

Fig. 10. Post-test conditions for Case 3.

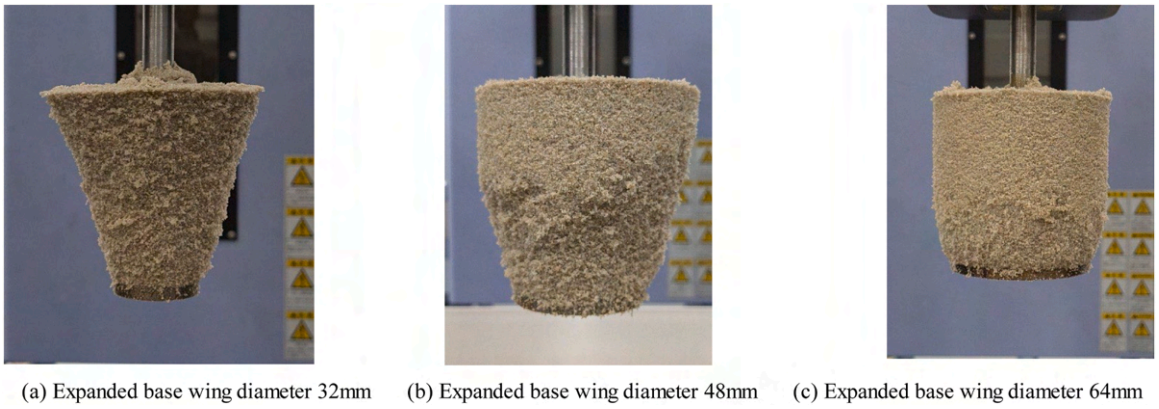

Fig. 11. Soil mass lifted by steel pipe piles.

beyond immediate base wing vicinity, with external soil participating through confinement effects on internal soil or through independent frictional contribution along steel structural member exterior surfaces.

Case 7 extends Case 6 by employing corrugated rather than smooth steel members, testing whether surface irregularity benefits persist under density differential conditions. Uplift forces of 17.20 N, 23.05 N, 22.82 N, 25.69 N, and maximum 31.14 N demonstrate approximately 12% enhancement compared to Case 6, closely matching the enhancement magnitude observed in Case 5 relative to Case 3. This consistency confirms that corrugated member benefits remain robust across varying soil density conditions, supporting specification of corrugated members as general practice rather than conditional on achieving high-quality soil compaction. The persistence of diameter-resistance relationships even under density differentials further validates fundamental design approaches while

highlighting the importance of considering external soil properties in capacity calculations.

4.6. Synthesis of experimental findings

Comprehensive analysis of all experimental configurations yielded several critical insights into the uplift resistance mechanisms of winged composite pile foundations. Uplift force was observed to increase consistently with the expanded base wing diameter across all seven test cases, irrespective of steel structural member presence, variations in soil density, or the application of surface corrugations. Fig. 9 demonstrates systematically that maximum resistance is positively correlated with wing diameter for all configurations, revealing this relationship as a fundamental design principle for such systems.

The test results confirmed that the incorporation of steel structural members enables winged composite piles to achieve uplift capacities comparable to, or surpassing, those of conventional steel pipe piles, provided that suitable conditions, particularly adequate soil compaction, are ensured. However, the performance of the composite system is strongly dependent upon both the physical properties of the contained and surrounding soil and the surface geometry of the steel member, suggesting that the steel structural members act mainly through confinement and friction rather than as simple additive resistive elements.

The effect of soil density proved pronounced: a 20% reduction in soil density resulted in an approximately 50% reduction in uplift capacity in all tested cases, as shown in Fig. 9. This finding highlights that strict quality control of soil compaction during surplus soil placement is paramount for ensuring the desired foundation performance in field conditions.

Surface irregularities, specifically, corrugated steel members, provided a consistent uplift resistance enhancement of approximately 12–13% over smooth members, independent of soil density. This enhancement is ascribed to increased soil–member interface area and mechanical interlocking, thus endorsing the selection of corrugated members (such as liner plates) for practical applications wherever feasible.

External soil conditions also influence uplift resistance, even where the primary uplift mechanism originates within the steel member/expanded base domain, as demonstrated by comparative analysis of Cases 3, 4, 6, and 7. Designers should, therefore, consider not only the properties of construction surplus soil inside structural members but also the characteristics of in situ ground outside the composite element.

Fig. 10 presents photographic documentation of the post-test conditions for Case 3, showing the deformed state of the contained soil mass after uplift. This image illustrates that the expanded base mobilizes the inner soil mass as a nearly rigid block during uplift, with significant resistance arising from friction along the interface between the steel member wall and the upward-moving soil. This visual evidence supports the mechanical interpretations of the observed load–displacement responses.

Fig. 11 further substantiates the uplift mechanism, displaying the extracted soil mass corresponding to multiple expanded base diameters. The images facilitate a direct assessment of how the size of the mobilized soil block increases with wing diameter, reinforcing the experimental observation that uplift capacity is governed not only by the physical dimensions of the steel elements but also by the extent of the soil mass that actively participates in resistance.

Collectively, these results, supported by photographic evidence from Figs. 10 and 11, provide robust empirical confirmation of the principal resistance mechanisms and parameter sensitivities discussed. They establish the core performance relationships necessary for the rational design and implementation of winged composite pile foundations utilizing construction surplus soil.

5. Numerical reproduction analysis and validation

5.1. Analysis objectives and approach

Numerical reproduction analyses using finite element method aim to validate experimental results and verify analytical methodology applicability for winged composite pile foundation design [35,36]. Three cases designated Case 3, Case 4, and Case 6 were selected for reproduction analysis based on their representation of key configurations: uniform high density, uniform low density, and density differential respectively. Analysis models replicate experimental dimensions exactly while material parameters derive from experimental conditions subject to necessary assumptions regarding unmeasured properties.

A critical methodological consideration warrants emphasis. Model experiments measured only soil unit weight directly, with detailed material constants including elastic modulus, shear modulus, cohesion, and internal friction angle remaining unmeasured due to specimen size limitations and testing scope constraints. Consequently, these parameters were estimated from assumed N-values using established correlations applicable to sandy soils [37,38]. This simplification necessarily introduces quantitative differences between experimental and analytical results. However, the analysis objective centers on confirming qualitative trend agreement, particularly regarding relationships between expanded base wing diameter and uplift force, rather than achieving precise numerical match. Successful qualitative agreement validates analytical methodology for parametric studies and design applications where relative performance comparisons guide decision-making.

5.2. Analysis conditions and parameters

Analysis model configuration replicates experimental soil container dimensions of 400 mm by 400 mm plan area extending 600 mm depth, with 300 mm pile length, 300 mm steel structural member length where applicable, and 100 mm steel member diameter as illustrated in Fig. 12. Mesh discretization employs refined elements near the expanded base wing where stress gradients concentrate, with progressive coarsening toward model boundaries where stress levels diminish. This adaptive meshing strategy balances computational efficiency against accuracy in regions governing system response.

In the numerical reproduction analyses, the soil domain is modeled with the same plan dimensions and depth as the experimental container. The steel structural member (liner plate) surrounding the steel pipe pile is also explicitly included. Under uplift loading, mobilized deformation and failure mechanisms concentrate within the soil mass inside the structural member and in the immediate vicinity of the expanded base wing. The outer region mainly provides global confinement, as observed in post-test photographs. Thus, the container walls and outer soil boundaries are represented by kinematic constraints (fixed bottom and normal lateral boundary restraints) to reproduce the experimental conditions. Their influence is interpreted as part of the composite confinement system rather than an artificial boundary effect to be eliminated. Since the tests and numerical models have the same geometric limits and boundary constraints, any boundary effect is present in both and does not affect the comparison of experimental and analytical results.

Prior to the final analyses, a mesh convergence assessment was conducted to confirm that the predicted uplift response was not overly sensitive to element size, especially near the expanded base wing, where stress gradients are concentrated. Three mesh configurations were examined: a coarse mesh with an average element size of approximately 15 mm around the expanded base wing; a medium mesh with an element size of about 10 mm; and a fine mesh with an element size of about 5 mm in the same region. In all cases, the mesh gradually became coarser toward the model boundaries. For Case 3, which had an expanded base wing of 64 mm, the maximum uplift force predicted by the medium and fine meshes differed by $<3\%$. The corresponding load–displacement

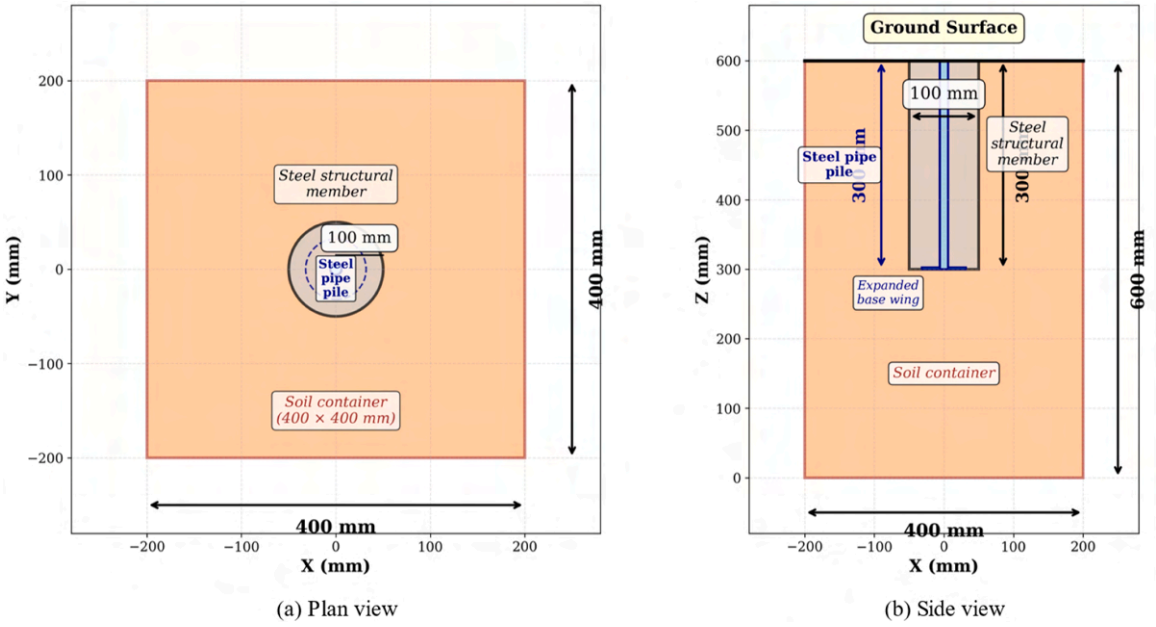

Fig. 12. Finite element analysis model configuration.

curves showed nearly identical shapes over the entire displacement range. Based on these results, the medium mesh was adopted for all subsequent analyses because it strikes a balance between computational efficiency and accuracy. This ensures a mesh-independent representation of uplift resistance characteristics relevant to design.

Soil parameters for Case 3 reproduction analysis appear in Table 2. Unit weight matches the experimental value of 15 kN/m^3 directly measured during test soil placement. Elastic modulus and shear modulus derive from assumed N-value correlations appropriate for medium-dense sand at this density, yielding values of 26,400 kN/m^2 and 9790 kN/m^2, respectively. Poisson's ratio of 0.35 represents typical sandy soil behavior. Internal friction angle of 30 degrees and cohesion of 1.25 kN/m^2 reflect medium-dense sand shear strength characteristics [39–41]. Steel pipe pile parameters including unit weight of 76.6 kN/m^3, elastic modulus of 205,000,000 kN/m^2, and Poisson's ratio of 0.30 represent standard structural steel properties.

The Case 4 reproduction analysis parameters, shown in Table 3, reduce the soil unit weight to 12 kN/m^3 to match the experimental loose sand condition. The elastic modulus (21,400 kN/m^2) and the shear modulus (7830 kN/m^2) were determined using the same N-value-based empirical correlations as in Case 3, but with a lower assumed N-value, which is representative of loose silica sand. The internal friction angle decreased from 30° to 25° to reflect the transition from medium-dense to loose sand. This is within the typical range reported in the literature for this sand type. Cohesion remained at 1.25 kN/m^2 because the sand is essentially cohesionless, and the small cohesion value is a numerical parameter rather than a measured quantity. These adjustments aim to capture the relative reduction in stiffness and strength associated with the lower density rather than reproduce exact measured values. Steel parameters remain identical to Case 3 as pile material properties remain unchanged across cases.

Table 2
Material parameters for Case 3 analysis.

(a) Model ground (soil) parameters

Parameter	Value	Parameter	Value
Unit weight (kN/m^3)	15.00	Poisson's ratio	0.35
Elastic modulus (kN/m^2)	2.64×10^4	Internal friction angle (°)	19.40
Shear modulus (kN/m^2)	9.79×10^3	S-wave velocity (m/s)	80.00
Cohesion (kN/m^2)	1.25	P-wave velocity (m/s)	166.50

(b) Steel pipe pile parameters

Parameter	Value
Unit weight (kN/m^3)	76.60
Elastic modulus (kN/m^2)	2.05×10^8
Shear modulus (kN/m^2)	7.9×10^7
Poisson's ratio	0.30

Table 3
Material parameters for Case 4 analysis.

(a) Model ground (soil) parameters

Parameter	Value	Parameter	Value
Unit weight (kN/m^3)	12.00	Poisson's ratio	0.35
Elastic modulus (kN/m^2)	2.14×10^4	Internal friction angle (°)	19.47
Shear modulus (kN/m^2)	7.83×10^3	S-wave velocity (m/s)	80.00
Cohesion (kN/m^2)	1.25	P-wave velocity (m/s)	166.50

(b) Steel pipe pile parameters

Parameter	Value
Unit weight (kN/m^3)	76.60
Elastic modulus (kN/m^2)	2.05×10^8
Shear modulus (kN/m^2)	7.9×10^7
Poisson's ratio	0.30

Case 6 reproduction analysis introduces dual soil regions with parameters detailed in Table 4. External soil employs 15 kN/m^3 density with elastic modulus of 41,940 kN/m^2, internal friction angle of 21.32 degrees, and other properties adjusted for this density level. Internal soil reduces to 12 kN/m^3 density with correspondingly reduced strength and stiffness parameters matching those employed in Case 4 analysis. This dual-region approach enables simulation of density differential effects observed experimentally.

The finite element model represents the experimental soil container as a deformable continuum, constraining its external boundaries to resemble the rigid acrylic walls used in the tests. The bottom boundary of the soil domain is fully fixed in all directions, preventing vertical and horizontal movement. This allows the base to behave as a rigid support, which is consistent with the base of the container in the experiments. The four lateral boundaries are restrained in the direction normal to each boundary plane, but remain free in the tangential directions. This allows for vertical settlement and uplift, while suppressing the outward lateral translation of the container walls.

Table 4
Material parameters for Case 6 analysis.

(a) Model ground (external soil - outside steel member) parameters			
Parameter	**Value**	**Parameter**	**Value**
Unit weight (kN/m^3)	15.00	Poisson's ratio	0.35
Elastic modulus (kN/m^2)	41.94×10^3	Internal friction angle (°)	21.32
Shear modulus (kN/m^2)	15.53×10^3	S-wave velocity (m/s)	100.80
Cohesion (kN/m^2)	1.25	P-wave velocity (m/s)	209.80
(b) Model ground (internal soil - inside steel member) parameters			
Parameter	**Value**	**Parameter**	**Value**
Unit weight (kN/m^3)	12.00	Poisson's ratio	0.35
Elastic modulus (kN/m^2)	21.14×10^3	Internal friction angle (°)	19.47
Shear modulus (kN/m^2)	7.83×10^3	S-wave velocity (m/s)	80.00
Cohesion (kN/m^2)	1.25	P-wave velocity (m/s)	166.50
(c) Steel Pipe Pile Parameters			
Parameter		**Value**	
Unit weight (kN/m^3)		76.60	
Elastic modulus (kN/m^2)		2.05×10^8	
Shear modulus (kN/m^2)		7.9 × 10^7	
Poisson's ratio		0.30	

Symmetry boundary conditions are then imposed on the symmetry planes so that normal displacements and shear stresses vanish appropriately. The steel pipe pile and the steel structural member are modeled as linearly elastic bodies tied to the surrounding soil at the base and in the radial direction. Relative slip is permitted only along the pile shaft–soil interface, where uplift shaft resistance develops. Contact between the soil and steel elements is simulated using a Coulomb-type frictional interface. In this interface, normal separation is permitted, but tangential shear is limited by a friction coefficient that corresponds to the assumed soil-steel interface friction angle.

Uplift loading is reproduced by prescribing a vertical displacement at the pile head node and incrementally increasing it up to the maximum experimental displacement of 20 mm. Reaction forces at the pile head are recorded to obtain the load-displacement relationship. All other degrees of freedom at the pile head are constrained to prevent rigid-body rotation, consistent with the experimental loading frame configuration. This displacement-controlled loading scheme ensures stable numerical convergence beyond peak resistance and enables direct comparison with experimental tests performed under displacement control.

5.3. Analysis results and experimental comparison

Case 3 reproduction analysis results appear in Fig. 13(a) comparing analytical predictions with experimental measurements across the full expanded base wing diameter range. Analysis generally predicts higher uplift forces than experiments measured, with 28.47 N analytical versus 36.61 N experimental at 32 mm diameter, progressing to 47.11 N analytical versus 53.92 N experimental at 64 mm diameter. The systematic offset between predictions and measurements likely reflects the incomplete material parameter replication, particularly elastic modulus and internal friction angle assumptions potentially exceeding actual test soil properties or boundary condition idealizations in the numerical model. However, the critical observation emerges that both experimental and analytical results demonstrate uplift force increasing with expanded base wing diameter, with similar rate of increase between the two datasets. This qualitative agreement validates the analytical methodology for parametric design studies despite quantitative offsets. Maximum absolute difference of 8.14 N represents approximately 12% deviation relative to experimental values, falling within acceptable ranges considering parameter estimation uncertainties.

Case 4 reproduction analysis shown in Fig. 13(b) reveals more substantial quantitative differences between analytical predictions and experimental measurements. Analytical results of 27.77 N, 31.07 N, 35.87 N, 40.17 N, and 44.91 N across the diameter range substantially exceed corresponding experimental values of 13.99 N, 17.58 N, 16.63 N, 17.45 N, and 19.32 N. The larger discrepancies for Case 4 compared to Case 3 suggest that material parameter assumptions introduce greater errors for loose sand conditions than for dense sand. Specifically, the assumed 25-degree internal friction angle may exceed actual test soil friction angle at 12 kN/m^3 density, or elastic modulus assumptions may prove overly stiff for this density level. Despite these quantitative differences, both analytical and experimental datasets show uplift force increasing with expanded base wing diameter, maintaining the qualitative agreement essential for validating analytical methodology. Maximum difference of 25.59 N represents more substantial 130% deviation, highlighting the importance of material characterization for quantitative predictions while confirming qualitative trend utility.

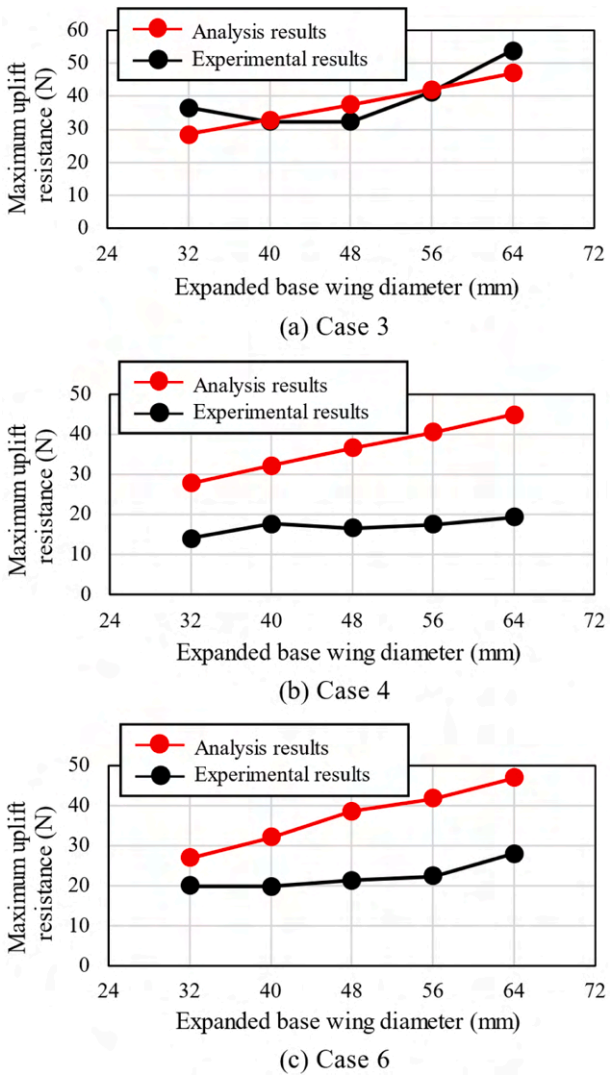

Fig. 13. Comparison of experimental and analytical results (Cases 3, 4, 6).

Case 6 reproduction analysis presented in Fig. 13(c) demonstrates intermediate behavior between Cases 3 and 4 regarding quantitative agreement. Analytical predictions of 26.82 N, 30.98 N, 33.26 N, 35.26 N, and 36.75 N compare with experimental measurements of 19.88 N, 19.62 N, 21.17 N, 22.22 N, and 27.85 N across the diameter range. Differences ranging from maximum 19.40 N to minimum 6.94 N prove smaller in both absolute and percentage terms than Case 4 discrepancies. This improved agreement for the density differential case suggests that material parameter estimation errors partially cancel when both high and low density regions contribute to overall response. The consistent increasing trend with diameter maintained

by both datasets confirms qualitative validation despite quantitative offsets.

5.4. Validation assessment and limitations

Fig. 14 comprehensively compares experimental and analytical results for expanded base wing diameter versus uplift force relationships across all three analyzed cases. Analysis results show similar magnitudes across cases, all confirming uplift force increase with expanded base wing diameter. The parallel trends between experimental and analytical datasets for each case validate the fundamental physical mechanisms captured by finite element modeling, including soil-structure interaction, bearing resistance mobilization, and frictional effects.

Critical evaluation of validation success requires acknowledging methodological limitations. Reproduction analyses match only unit weight to experimental values precisely, with all other parameters calculated from assumed N-values rather than direct measurement. This approach proves necessary given specimen size limitations in model-scale experiments but inevitably introduces parameter uncertainty. Quantitative experimental-analytical discrepancies ranging from 15% for dense uniform soil to 130% for loose uniform soil reflect this uncertainty, establishing that current analytical models cannot predict absolute capacities reliably without comprehensive material characterization. However, the consistent qualitative trend agreement across varying density conditions and steel member configurations demonstrates that analytical models capture fundamental behavior correctly.

The validation objective centers on confirming that experimental and analytical results exhibit similar trends in expanded base wing diameter versus uplift force relationships rather than achieving numerical precision. Successful confirmation of qualitative agreement across all three analyzed cases provides important evidence supporting numerical analysis-derived knowledge reliability. This validation enables confident application of numerical modeling for parametric design studies, comparative evaluations of alternative configurations, and optimization analyses where relative performance governs decisions. The established limitations regarding absolute capacity prediction emphasize the importance of field-scale verification testing before relying on numerical predictions for final design without empirical validation.

6. Design guidelines for winged composite pile foundations

6.1. Integrated design methodology

Design guidelines for winged composite pile foundations must integrate knowledge from numerical analyses and model experiments into a systematic methodology accessible to practicing engineers [42,43]. Fig. 15 presents the recommended design parameter determination sequence, which proceeds through the following steps:

(1) Pile Length and Steel Structural Member Diameter Determination: Determine pile length and steel structural member diameter based on ground conditions at the construction site and the type and scale of structure requiring support. Required uplift resistance relates approximately proportionally to pile length, enabling reverse calculation from structural loading demands to necessary embedded length.
(2) Shaft Diameter Determination: Determine shaft diameter ensuring adequate working space (minimum 60 cm clearance) for workers accessing the internal space between the steel pipe pile and steel structural member for surplus soil placement and compaction operations. Since shaft diameter exerts minimal influence on uplift resistance, prioritize constructability and economy.
(3) Expanded Base Wing Diameter Determination: Using numerical analysis relationships between pile length and uplift force, supplemented by shaft diameter effects, optimize expanded base wing dimensions for the established pile geometry. Optimal expanded base wing diameter typically ranges from 80% to 90% of steel structural member diameter, balancing capacity enhancement against construction complexity.
(4) Strength Enhancement Zone Determination: Determine the vertical extent over which construction surplus soil near the expanded base wing receives treatment with cement-based solidification agents. Model experiments and numerical analyses indicate that enhancement zones extending 20% to 30% of pile length upward from the expanded base wing provide optimal benefit.
(5) Solidification Material Selection: Select solidification agent type and quantity required to enhance steel structural member base interior soil to specified strength (N-value 10–15) based on site-specific construction surplus soil characteristics determined through laboratory testing programs.
(6) Steel Structural Member Selection: Specify member type and surface characteristics. Corrugated members such as liner plates enhance uplift resistance by 12% to 13% compared to smooth members. Economic analyses should compare total installed costs against capacity benefits to guide optimal member selection.

6.2. Critical design considerations

Several critical considerations transcend the sequential design methodology, requiring attention throughout the design process:

- Soil Compaction Quality Control: Construction specifications must establish clear density requirements with verification testing

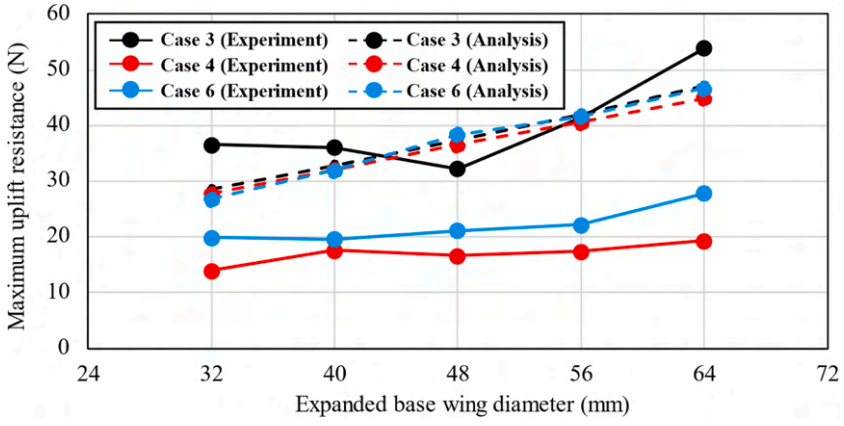

Fig. 14. Comprehensive comparison of all analytical and experimental results.

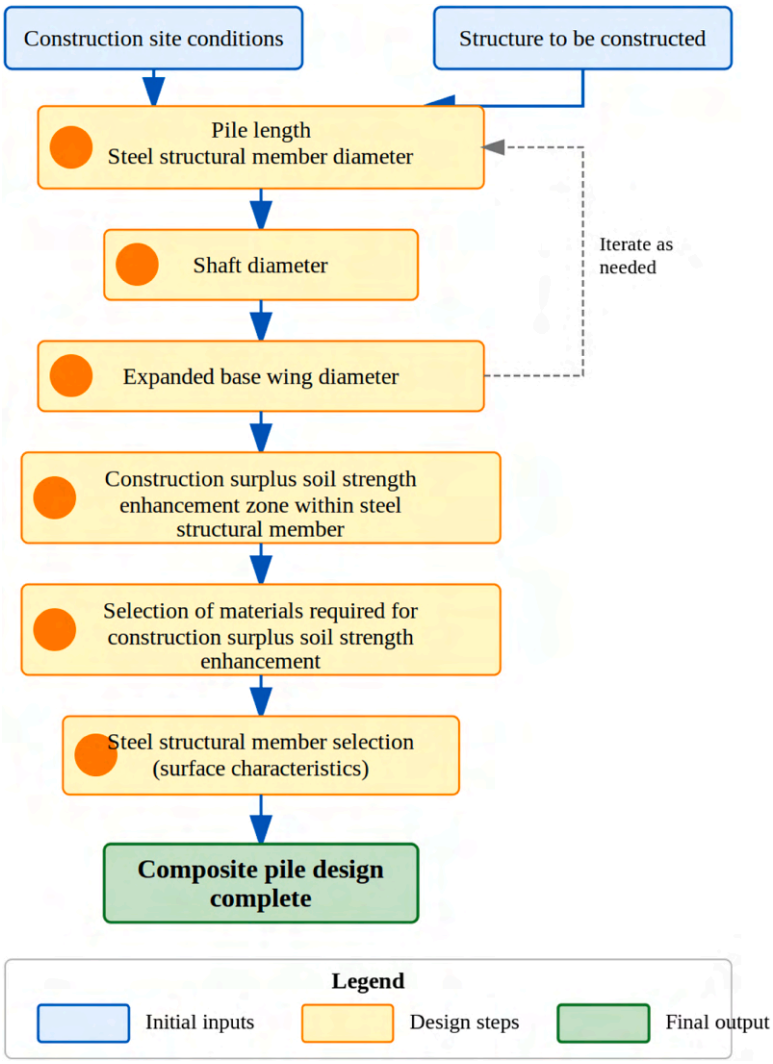

Fig. 15. Design guideline flowchart for winged composite pile foundations.

protocols ensuring achievement throughout the fill height, as 20% density reduction causes approximately 50% uplift resistance reduction. Compaction effort specifications should account for layer thickness, equipment type, and soil moisture content, with field density testing confirming compliance at regular intervals.

- External Soil Condition Effects: Design calculations should conservatively evaluate both best-case and worst-case external soil scenarios, particularly when site investigations reveal variable conditions or groundwater fluctuations that may alter soil properties during structure service life. External soil conditions beyond steel structural member boundaries influence overall system performance.
- Construction Quality Assurance: Quality assurance extends beyond density verification to encompass alignment control, with pile verticality maintained within 1% tolerance; member installation verification confirming depth, diameter, and wall integrity; and admixture placement documentation when solidification agents are specified.

7. Conclusions

7.1. Study achievements

This study has experimentally and numerically evaluated uplift resistance characteristics of winged composite pile foundations utilizing construction surplus soil through a comprehensive program comprising 35 model experiments and finite element method reproduction analyses of three selected cases. Principal achievements include:

(1) Universal diameter-resistance relationship: Uplift force increases with expanded base wing diameter across all test cases, remaining consistent regardless of steel structural member presence, soil density variations, or steel member surface irregularities. This fundamental relationship establishes a primary design principle applicable across the full range of practical configurations.
(2) Composite system validation: Winged composite piles incorporating installed steel structural members achieved uplift resistance comparable to or exceeding steel pipe piles alone under appropriate conditions, validating the proposed system concept for practical structural applications.
(3) Soil density sensitivity quantification: 20% soil density reduction from 15 to 12 kN/m^3 resulted in approximately 50% uplift force reduction, demonstrating that construction surplus soil compaction management during field construction proves essential for achieving design performance.
(4) Surface treatment effectiveness: Corrugated steel structural members enhanced uplift resistance by approximately 12% to 13% compared to smooth members across varying density conditions, validating the effectiveness of using corrugated steel members such as liner plates in actual winged composite pile foundations.

(5) Numerical methodology validation: Model experiments and reproduction analyses showed similar trends in expanded base wing diameter versus uplift force relationships, validating finite element methodology appropriateness for parametric design studies despite quantitative differences attributable to material parameter estimation uncertainty.
(6) Practical design framework: Integrated design guidelines were developed synthesizing knowledge from numerical analyses and model experiments, providing practicing engineers with accessible methodologies for implementing winged composite piles in appropriate applications.

7.2. Engineering significance and broader implications

This study addresses dual imperatives confronting contemporary geotechnical engineering practice. From a structural performance perspective, the work demonstrates that winged composite pile foundations can reliably achieve required uplift resistance for wind-load-resistant structures through systematic design considering expanded base wing dimensions, soil density specifications, and steel member surface characteristics. The quantitative relationships established between design parameters and resistance enable rational capacity predictions with appropriate consideration of parameter uncertainties and construction quality variability.

From an environmental sustainability perspective, the study provides a viable technological pathway for substantially increasing on-site utilization of construction surplus soil, potentially improving current 54.3% on-site utilization rates toward the 79.8% effective utilization target established in national policy objectives. The transformation of surplus soil from waste material requiring costly disposal into structural foundation elements supporting critical infrastructure represents a paradigm shift in construction waste management philosophy. Economic analyses at project scale should evaluate cost savings from avoided disposal against potential incremental costs for enhanced quality control, with many applications likely demonstrating net economic benefit alongside environmental advantages.

The validated experimental-numerical framework enables rational design decisions for winged composite pile foundation systems while facilitating technology transfer from study to practice. Design guidelines developed through this work provide practicing engineers with accessible methodologies for implementing winged composite piles in appropriate applications without requiring specialized expertise in study-level computational modeling or advanced soil mechanics.

7.3. Future study directions

Several important study questions remain unresolved, requiring investigation before complete confidence in field-scale implementation can be established:

(1) Soil type variations: Model experiments employed only silica sand as test soil. Study investigating various construction surplus soil types with different grain size distributions, plasticity indices, and gradation characteristics would establish performance relationships across the full spectrum of materials likely encountered in practice. Particular attention should focus on cohesive soils where time-dependent consolidation behavior and moisture sensitivity may substantially influence both construction procedures and long-term performance.
(2) Full-scale field testing: Full-scale field tests represent an essential validation step. Model experiments necessarily introduce scale effects that may cause behavioral differences from full-scale applications, particularly regarding soil dilatancy, particle crushing, and strain localization phenomena. Field test programs should instrument full-scale winged composite pile foundations during installation and loading to verify that mechanisms observed at model scale remain operative at prototype scale.
(3) Dynamic loading considerations: Study addressed only static uplift loading, while actual wind loads possess time-varying characteristics with potential for cyclic loading effects, dynamic amplification, and resonance phenomena. Study programs should examine winged composite pile response under cyclic loading protocols representative of wind storm load histories.
(4) Long-term performance assessment: Long-term loading tests would evaluate creep characteristics and assess deformation progression under constant uplift force application representing steady wind loads. Time-dependent behavior of construction surplus soil under sustained stress may differ substantially from short-term monotonic loading response captured in model experiments.
(5) Construction quality assurance procedures: Laboratory-derived compaction specifications and density requirements must translate to practical field procedures executable with available equipment under actual site constraints. Study integrating construction engineering perspectives with geotechnical design considerations would establish optimal construction sequences and effective verification testing protocols.
(6) Economic optimization analyses: Cost modeling should comprehensively account for material costs, construction labor and equipment, quality control and verification testing, and avoided disposal fees. Decision frameworks integrating economic, environmental, and technical performance considerations would enable stakeholders to make informed technology adoption decisions for specific projects.

7.4. Implementation strategy and path forward

Addressing these study directions requires coordinated efforts among multiple stakeholders including researchers, consulting engineers, contractors, and regulatory agencies. A phased implementation strategy would proceed as follows:

- Phase 1 (Pilot Projects) Begin with pilot projects at carefully selected sites offering favorable soil conditions and manageable risk levels to generate field experience while minimizing consequences of unforeseen issues. Early projects should incorporate comprehensive instrumentation and monitoring programs generating data to validate design methodologies.
- Phase 2 (Knowledge Dissemination): Professional education initiatives introducing winged composite pile foundation concepts to practicing engineers through technical publications, conference presentations, and continuing education programs would accelerate knowledge dissemination and technology transfer.
- Phase 3 (Regulatory Framework Development): Regulatory engagement with building code authorities and geotechnical design standard committees would establish appropriate design factors, quality assurance requirements, and approval processes for winged composite pile foundations.
- Phase 4 (Broad Adoption): Experience accumulated through early implementations would inform evidence-based regulatory provisions balancing innovation encouragement with public safety protection, enabling confident widespread adoption.

This comprehensive implementation strategy progressing from fundamental study through pilot applications to broad adoption would realize the full potential of winged composite pile foundations for addressing both structural performance requirements and construction waste management challenges. The technology offers genuine promise for advancing sustainable construction practices while meeting increasing demands for resilient infrastructure capable of withstanding intensifying climate-driven environmental loads.

CRediT authorship contribution statement

Shinya Inazumi: Writing – review & editing, Writing – original draft, Visualization, Supervision, Resources, Methodology, Funding acquisition, Formal analysis, Conceptualization. **Yusuke Watanabe:** Validation, Resources, Investigation. **Yosuke Mizutani:** Validation, Resources, Methodology, Investigation, Data curation. **Yoshihiro Matsuo:** Validation, Resources, Investigation. **Ken-ichi Shishido:** Visualization, Resources, Methodology.

Declaration of competing interest

The authors declare that they have no known competing financial interests or personal relationships that could have appeared to influence the work reported in this paper.

Data availability

Data will be made available on request.

References

[1] S. Wang, S. Ke, Y. Zhao, Y. Yun, W. Zhang, J. Yang, H. Ren, Research on hydrodynamics of foundation structure of offshore wind turbine under typhoon-wave-current coupling, Adv. Struct. Eng. 25 (12) (2022) 2558–2576, https://doi.org/10.1177/13694332221104283.

[2] P. Li, Y. Zhang, Z. Wang, Y. Teng, J. Yi, T. Mu, J. Wu, Q. Wu, Development of design typhoon profile for offshore wind turbine foundation design in Southern China, Mar. Struct. 88 (2023), https://doi.org/10.1016/j.marstruc.2023.103479. Article 103479.

[3] Z. Hu, S. Qu, Q. Wang, Y. Guo, Y. Ji, Pullout behaviour of belled piles under axial and oblique pull in soil-rock composite ground: an experimental study, Int. J. Civ. Eng. 21 (2022) 569–582, https://doi.org/10.1007/s40999-022-00778-1.

[4] Y. Li, H. Zhang, Analysis of wind-induced vibration response of distribution line concrete poles with pedestal piles, Proc. SPIE 13513 (2025), https://doi.org/10.1117/12.3056678, 1351346–1–1351346–7.

[5] A. Agarwal, H. Irtaza, M. Khan, Experimental study of pulling-out capacity of foundation for solar array mounting frames, Indian Geotech. J. 51 (3) (2020) 414–420, https://doi.org/10.1007/s40098-020-00456-w.

[6] Kamon, M., & Katsumi, T. (2021). Civil engineering use of industrial waste in Japan. In Developments in Geotechnical Engineering. 10.1201/9781003211013-23.

[7] S. Inazumi, M. Shiina, K. Nakao, Aeration curing for recycling construction-generated sludge and its effect of immobilizing carbon dioxide, Case Stud. Construct. Mater. 20 (2024), https://doi.org/10.1016/j.cscm.2023.e02704. Article e02704.

[8] H. Ito, H. Masuda, A. Oshima, Leaching characteristics of naturally derived toxic elements in the alluvial marine clay layer beneath Osaka Plain, Japan: implications for the reuse of excavated soils, Environ. Earth. Sci. 78 (2019), https://doi.org/10.1007/s12665-019-8595-3. Article 459.

[9] S. Hale, A. Roque, G. Okkenhaug, E. Sørmo, T. Lenoir, C. Carlsson, D. Kupryianchyk, P. Flyhammar, B. Zlender, The reuse of excavated soils from construction and demolition projects: limitations and possibilities, Sustainability 13 (11) (2021), https://doi.org/10.3390/su13116083. Article 6083.

[10] H. Choi, M. Park, D. Jeong, J. Kim, Soil recycling among construction sites by optimizing schedule and costs for earthmoving, J. Asian Archit. Build. Eng. 16 (3) (2017) 439–446, https://doi.org/10.3130/jsaabe.16.439.

[11] P. Minixhofer, B. Scharf, S. Hafner, O. Weiss, T. Room, R. Stangl, Towards the circular soil concept: optimization of engineered soils for green infrastructure application, Sustainability 14 (2) (2022), https://doi.org/10.3390/su14020905. Article 905.

[12] M. Islam, S. Turja, D. Van Nguyen, D. Kim, Lateral response and failure mechanism of single and group piles in cement-improved soil, Results Eng. 22 (2024), https://doi.org/10.1016/j.rineng.2024.102668. Article 102668.

[13] Z. Yang, K. Chen, X. Fu, Z. Zou, Effects of cement-enhanced soil on the ultimate lateral resistance of winged composite pile in clayey soil, J. Rock Mech. Geotech. Eng. 15 (3) (2023) 1–10, https://doi.org/10.1016/j.jrmge.2023.03.010.

[14] J. Zhou, X. Gong, K. Wang, R. Zhang, J. Yan, Testing and modeling the behavior of pre-bored grouting planted piles under compression and tension, Acta Geotech. 12 (5) (2017) 1061–1075, https://doi.org/10.1007/s11440-017-0540-6.

[15] Q. Zhang, H. Deng, W. Yi, G. Dai, H. Li, X. Guo, Study on uplift mechanism of grouted implantation steel pipe pile by direct shear and model tests, Soils Found. 64 (3) (2024), https://doi.org/10.1016/j.sandf.2024.101459. Article 101459.

[16] A. Sharma, A. Kumari, A. Alsabhan, S. Alam, K. Singh, A. Tiwary, J. Qadri, A. Senagah, G. Juneja, R. Gupta, A. Mehta, Optimization of steel anchor pile configurations for enhanced pullout resistance in expansive soil foundations, Sci. Rep. 15 (2025), https://doi.org/10.1038/s41598-025-13353-0. Article 13353.

[17] T. Pei, T. Qiu, A numerical investigation of laterally loaded steel fin pile foundation in sand, Int. J. Geomech. 22 (6) (2022), https://doi.org/10.1061/(asce)gm.1943-5622.0002417. Article 04022060.

[18] J. Peng, Y. Miyazaki, Experimental study on unique interactions in steel pipe sheet piles under lateral load: joint, pipe, and soil, Acta Geotech. 20 (1) (2025) 123–137, https://doi.org/10.1007/s11440-025-02536-8.

[19] H. Malhotra, S. Singh, Experimental and numerical studies on uplift behavior of granular anchor pile foundation embedded in sandy soil, Arab. J. Sci. Eng. 46 (5) (2020) 4477–4487, https://doi.org/10.1007/s13369-020-05013-4.

[20] M. Shaheen, M. Rabei, M. Mansour, A. El-Deen, The influence of soil reinforcement on the performance of single pile and pile group under pullout loads, Eng. Res. J. (2024), https://doi.org/10.21608/erj.2024.377302.

[21] J. Kim, U. Kim, B. Min, H. Choi, S. Park, Development of expanded steel pipe pile to enhance bearing capacity, Sustainability 14 (5) (2022), https://doi.org/10.3390/su14053077. Article 3077.

[22] H. Bao, J. Peng, Z. Cheng, J. Hong, Y. Gao, Experimental study on inner interface mechanical properties of the ESDCM pile with steel core, Buildings 13 (2) (2023), https://doi.org/10.3390/buildings13020486. Article 486.

[23] I. Umar, M. Firat, H. Lin, H. Shehu, R. Cao, Performance analysis of hybrid steel–concrete and timber–concrete winged composite pile systems in variable density sandy soils using experimental and numerical insights, Appl. Sci. 15 (11) (2025), https://doi.org/10.3390/app15115868. Article 5868.

[24] X. Wang, Q. Pei, Field tests and the numerical analysis of a pile-net composite foundation for an intelligent connected motor-racing circuit, Buildings 14 (1) (2024), https://doi.org/10.3390/buildings14010174. Article 174.

[25] A. Derlatka, S. Labocha, P. Lacki, The load-bearing capacity assessment of GFRP foundation piles for transmission line poles using experimental tests and numerical calculations, Appl. Sci. 15 (4) (2025), https://doi.org/10.3390/app15042231. Article 2231.

[26] F. Al-Darraji, M. Sadique, Z. Yu, A. Shubbar, T. Čebašek, Performance of confined concrete-filled aluminum tube pile groups under combined loading, Geotech. Geol. Eng. (Dordr) (2025), https://doi.org/10.1007/s10706-024-03002-0.

[27] F. Tehrani, F. Han, R. Salgado, M. Prezzi, R. Tovar, A. Castro, Effect of surface roughness on the shaft resistance of non-displacement piles embedded in sand, Geotechnique 66 (5) (2016) 386–400, https://doi.org/10.1680/jgeot.15.p.007.

[28] B. Uge, Y. Guo, CFG pile composite foundation: its engineering applications and research advances, J. Eng. 2020 (2020), https://doi.org/10.1155/2020/5343472. Article 5343472.

[29] Z. Jin, G. Fang, S. Zhao, Engineering design and static load test of soil filling pile with spiral cone foundation, in: Proceedings of the IOP Conference Series: Earth and Environmental Science 687, 2021, https://doi.org/10.1088/1755-1315/687/1/012111. Article 012111.

[30] G. Chen, H. Yu, A. Bobet, Analytical solution for seismic response of deep tunnels with an arbitrary cross-section and voids behind the liner, Rock. Mech. Rock. Eng. 56 (2023) 1–17, https://doi.org/10.1007/s00603-023-03323-1.

[31] N. Seregin, An integrated way to improve the properties of soil-cement pile foundations, in: Proceedings of the E3S Web of Conferences, 2020, p. 157, https://doi.org/10.1051/e3sconf/202015706006. Article 06006.

[32] R. Dingcong, A. Cavero, K. Pantaleon, F. Maravillas, M. Ahalajal, E. Cea, L. Mendija, K. Tejas, S. Manlupig, R. Malaluan, A. Lubguban, Enhanced soil piles with Portland cement-RHA-MWCNT mix for deep mixing methods in low-rise building and bridge foundations, ASEAN Eng. J. 15 (2025), https://doi.org/10.11113/aej.v15.21897. Article 21897.

[33] Z. Xue, W. Zhang, X. Zhao, F. Meng, F. Qin, G. Xiao, Z. Nie, J. Chen, Utilization of cement deep mixing pile for soft soil foundation: a Malaysian case study, Front. Mater. (2024), https://doi.org/10.3389/fmats.2024.1484228.

[34] O. Al-Ketan, R. Al-Rub, R. Rowshan, Mechanical properties of a new type of architected interpenetrating phase composite materials, Adv. Mater. Technol. 2 (6) (2017), https://doi.org/10.1002/admt.201600235. Article 1600235.

[35] S. Sui, X. Zhang, K. Lu, Z. Li, W. Liu, H. Xu, P. Han, Finite element analysis of combined bearing characteristics of pile–soil interaction in composite foundation, Appl. Sci. 14 (9) (2024), https://doi.org/10.3390/app14093894. Article 3894.

[36] R. Lang, H. Xiong, L. Sun, Z. Yadong, A simplified prediction method for additional stress on underlying layer of rigid pile-net composite foundation, Eur. J. Environ. Civ. Eng. 26 (17) (2021) 5696–5715, https://doi.org/10.1080/19648189.2021.1916603.

[37] M. Hatanaka, A. Uchida, Empirical correlation between penetration resistance and internal friction angle of sandy soils, Soils Found. 36 (4) (1996) 1–9, https://doi.org/10.3208/sandf.36.4_1.

[38] B. Ghoreishi, M. Esfahani, N. Lushabi, O. Amini, I. Aghamolaie, N. Hashim, S. Alizadeh, Assessment of geotechnical properties and determination of shear strength parameters, Geotech. Geol. Eng. (Dordr) 39 (1) (2020) 461–478, https://doi.org/10.1007/s10706-020-01504-1.

[39] X. Yin, Application of Poisson effect in rock and soil mass, J. Phys. Conf. Ser. 3005 (1) (2025), https://doi.org/10.1088/1742-6596/3005/1/012004. Article 012004.

[40] K. Żarkiewicz, R. Bednarek, Shear strength of sand: integrated analysis of initial porosity and stress effects, Appl. Sci. 15 (11) (2025), https://doi.org/10.3390/app15115902. Article 5902.

[41] D. Bouri, A. Krim, A. Brahim, A. Arab, Shear strength of compacted Chlef sand: effect of water content, fines content and other parameters, Stud. Geotech. Mech. 42 (1) (2020) 18–35, https://doi.org/10.2478/sgem-2019-0027.
[42] T. Yang, W. Zheng, Y. Xie, H. Zhang, X. Yue, Evaluating screw-shaft pile composite foundations in round gravelly soil: a study using model tests and numerical simulations, Heliyon 9 (7) (2023) e20887, https://doi.org/10.1016/j.heliyon.2023.e20887.
[43] X. Wang, Z. Feng, S. Wang, W. Wang, Experimental study and numerical simulation of the effect of rigid pile composite foundations on slab culverts, Adv. Civ. Eng. 2023 (2023), https://doi.org/10.1155/2023/4778445. Article 4778445.